Mixing models in close-range spectral imaging for pigment mapping in Cultural Heritage

Federico Grillini*, Jean-Baptiste Thomas, Sony George

The Norwegian Colour and Visual Computing Laboratory, NTNU-IDI, Gjøvik, Norway
*Corresponding author: federigr@ntnu.no

ABSTRACT

Pigment mapping is a fundamental tool in the field of conservation of cultural heritage paintings. It allows the identification of the pigments, their estimation of their relative concentrations, and their monitoring. In this work, we propose and analyze the spectral unmixing performances of seven optical mixing models, in order to understand which one is the most suited in a possible real-case application. Using a pigments palette inspired by the Renaissance period, we realize a set of mock-ups to test the models. The best results are obtained with models with a subtractive nature. The purely subtractive model is then tested on a case-study painting performed with the same set of pigments, in order to produce concentration maps related to each one of the primaries.

KEYWORDS
pigment mapping **I** *cultural heritage* **I** *optical model* **I** *spectral unmixing*

INTRODUCTION

The conservation of Cultural Heritage (CH) is considered paramount by modern society since it enables the communities to learn from the past and transmit the important values of traditions and arts to the next generations. CH artefacts are to be preserved in the best conditions as possible, but also they have to be studied, to understand the techniques and procedures that the Old Masters were adopting. During the inspection of such sensitive objects, *non-invasive* and *non-destructive* techniques must be prioritized. Many non-contact analytical and imaging techniques have been deployed for the study of CH artefacts. García-Bucio *et al.* (2016) exploited Raman Spectroscopy to assess the material composition of the pictorial layer of paintings. Particles Induced X-ray Emission (PIXE) can be used to investigate the layered structures of paintings, as demonstrated by Grassi *et al.* (2005). The composition of an artefact can also be studied via X-Ray Fluorescence (XRF), as in the work of Mantler and Schreiner (2000). The properties of the binding media commonly used in oil painting can be investigated using Fourier Transform Infra-Red (FTIR), as Sotiropoulou *et al.* (2016) report in their research. Optical Coherence Tomography (OCT) is an imaging technique that enables the analysis of scarcely opaque objects and can find applications in the field of CH, as demonstrated by Targowski and Iwanicka (2012).

In this study we focus on oil paintings, using as imaging technique Hyper Spectral Imaging (HIS), which allows the user to reach high levels of resolution in the spatial and spectral dimensions. HSI can be helpful in tackling several applications regarding oil painting, such as the monitoring of artefacts and the assessment of the pictorial technique. Strojnik *et al.* (2011) showed how HSI can be used to investigate the presence of hidden layers or *pentimenti* in paintings, exploiting the transparency properties of pigments in the Infra-red region of the electromagnetic spectrum. By combining the spectral information obtained at a quasi-microscopic level, it is possible to study tiny areas of the painting in order to learn their composition in terms of pigments used. This task is known as Pigment Mapping (PM). Deborah *et al.* (2014) performed pigment identification and PM on the renowned painting *The Scream*. The task of PM is a specific application of what in remote sensing is known as Spectral Unmixing (SU). An exhaustive review of SU methods is proposed by Bioucas-Dias *et al.* (2012).

The aim of SU is to *decompose* a spectrum into several pure spectra, denominated *endmembers* or *primaries*. Each endmember is also associated with a concentration ratio, included in the interval [0,1]. When a spectrum is decomposed, the resulting concentrations must add up to the unit, besides being all positive numbers. Lastly, in order to decompose a spectrum, a mixing model needs to be defined and inverted. The aim of this research work is to define a series of mixing models and to invert them on oil painting targets prepared for the occasion (*mock-ups*). The model that results the best in estimating the concentrations of the mock-ups is then inverted and validated on a case-study painting to perform pigment mapping.

Optical Mixing Models

The reflectance factors $\rho(\lambda)$ of several materials can be combined in order to output a resulting reflectance factor that carries information about each component. The interaction between reflectance spectra is modulated by an optical mixing model. Such a model also requires the knowledge of a concentration vector **C** = $\{\alpha_1, \alpha_2, \ldots, \alpha_v\}$ in which all elements comply with non-negativity and sum-to-one constraints. The endmembers are stored in a matrix ***E*** of dimensions λ (number of spectral bands) by *q* (number of endmembers) and are combined with **C** to produce a resulting vector ***Y***:

$$Y_{[\lambda \cdot 1]} = f(E_{[\lambda \cdot q]}, C_{[q \cdot 1]}) \quad (1)$$

The investigated mixing models are a subset of those studied by Grillini *et al.* (2020) and are reported in Tab. 1. In order to retrieve the concentration vector, the models are inverted using the optimization process for non-linear constrained functions introduced by Nelder and Mead (1965). The adopted cost function aims to maximize the Peak Signal-to-Noise Ratio (PSNR) between the reference spectrum and the target one Y. The assumption we formulate is that if the produced spectrum is very close to the reference, then the concentration vector would approach the ground truth as well.

EXPERIMENTS

A set of 175 mock-ups (Fig. 1a) is realized using a palette of pigments provided by Kremer Pigmente GmbH \& Co.KG Inc. that included: Kremer White (W), Ultramarine Blue (B), Naples Yellow (Y), Gold Ochre DD (O), Viridian Green (G), Novoperm Carmine Red (C) and Vermilion (V). The support used for the occasion was canvas, primed with a layer of Kremer Gesso, while the binding medium was linseed oil. For each patch, the pigments were weighted to obtain an accurate concentration ground truth. Only mixtures containing up to 3 pigments were included in this study. With the same set of pigments, a case-study painting depicting the famous *Baby Yoda meme* (Fig. 1b), was realized for the occasion. In this painting, 12 areas with a known concentration vector, are identified and used as targets for the unmixing task.

Label	Name	Equation	Category
M_1	Additive	$Y=\sum_{i=1}^{N}\rho_i\alpha_i$	A
M_2	Subtractive (Burns 2017)	$Y=\prod_{i=1}^{N}\rho_i^{\alpha_i}$	S
M_3	LIP additive	$Y=1-\prod_{i=1}^{N}(1-\rho_i)^{\alpha_i}$	A
M_4	LIP subtractive	$Y=1-exp\left[-\prod_{i=1}^{N}[-log(1-\rho_i)]^{\alpha_i}\right]$	S
M_5	Yule-Nielsen (1951)	$Y=\left(\sum_{i=1}^{N}\alpha_i\rho_i^{\tau}\right)^{\frac{1}{\tau}}$	H
M_6	Add-Sub (Simonot and Hébert 2014)	$Y=\tau\sum_{i=1}^{N}\alpha_i\rho_i+(1-\tau)\prod_{i=1}^{N}\rho_i^{\alpha_i}$	H/A
M_7	Sub-Add (Simonot and Hébert 2014)	$Y=\left(\sum_{i=1}^{N}\alpha_i\rho_i^{\tau}\right)\left(\prod_{i=1}^{N}\rho_i^{\alpha_i(1-\tau)}\right)$	H/S

Tab. 1 Studied optical mixing models divided into three main categories: additive (A), subtractive (S) and hybrid (H). The models M6 and M7 are indeed hybrid but have strong additive and subtractive tendencies, respectively. Models M3 and M4 are obtained adapting M1 and M2 to the rules of the Logarithmic Image Processing developed by Jourlin and Pinoli (2001).

(a) (b)

Fig. 1 (a): Set of mock-ups realized for the experiment. 175 patches report different concentration ratios for 7 pigments. Each mock-up has a size of 2x2 cm, a dimension that is easily captured by the HS camera at a high resolution. (b): RGB image of the painting. The image is obtained after HS scanning, computing the RGB colors assuming a standard illuminant D65. 12 macro-areas with approximated known concentrations are highlighted.

All the targets presented in this study were captured with a push-broom HySpex VNIR-1800 hyperspectral camera produced by Norsko Elektro Optikk. This line scanner deploys a diffraction grating and results in generating 186 images across the electromagnetic spectrum, from *400nm* to *1000nm*, at steps of approximately *3.19nm*. The focus of the optics is set to *30cm*. At each acquisition, a Spectralon® calibration target with a known wavelength-dependent reflectance factor is included in the scene. The target will serve to estimate the illuminant spectrum and to compute the reflectance factor at the pixel level.

We understand that this process assume a linear optical mixing model, which may not describe well our object, but this is a very accepted process and in our case the working with normalized radiance or reflectance factors is equivalent. Radiometric correction and flat field corrections are performed as post-processing steps, following the recommendations of George *et al.* (2018) and Pillay *et al.* (2019).

RESULTS AND DISCUSSION

We opted to use a new metric that could combine the accuracies of spectral reconstruction and concentration to evaluate the unmixing performances when the mockups are used as targets. The new metric w is defined as follows:

$$w=100/PSNR\ \Delta\alpha \quad (2)$$

in which $\Delta\alpha$ represents the Euclidean distance between the ground truth concentration vector and the estimated one. As w takes on smaller values, the accuracy increases. Tab.2 reports some statistics concerning this newly introduced metric for each one of the proposed models. From this data, we can state that the model that describes best the mixing of pigments in oil painting is the purely subtractive model M_2.

	M_1	M_2	M_3	M_4	M_5	M_6	M_7
Mean	1.46	**1.13**	1.58	**1.15**	1.27	1.30	**1.19**
Max	2.54	2.51	2.78	2.44	2.51	2.52	2.51
Std Dev	0.50	0.49	0.50	0.47	0.49	0.50	0.49

Tab. 2. Results of the new metric w. Smaller values indicate better estimation, therefore subtractive-based models (highlighted in bold) are to be preferred.

Case - study

The case-study painting of Baby Yoda is captured in the HS set-up and then processed with the SuperPixel SLIC algorithm developed by Achanta *et al.* (2012), in order to reduce the number of data-points that need to be investigated. Amongst the 2000 super-pixels, 12 of them are selected to represent the 12 macro-areas in which the pigments and their relative ratios are known. Tab. 3 reports the analysis of such areas. The estimated labels are assigned with the following rules: a letter appears if the relative concentration is at least 15%, while a capital letter is given with concentrations ≥ 30%. Some pigments are harder to detect (Naples Yellow, Carmine), making the labeling task a complex problem with room for improvement. Fig. 2 shows the concentration maps for each pigment, when the subtractive model M2 is inverted. From a visual standpoint, the maps are a quite faithful representation of reality, except for some instances. Ultramarine Blue is used only for the sky portion of the painting, but was nonetheless detected in significative amounts in other areas. There is probably a difficulty in differentiating between Gold Ochre DD and Naples Yellow, with the former being largely selected. Viridian Green is also detected in the sky, where only Blue and White are used. On the other hand, the mapping of Vermilion, Kremer White and Novoperm Carmine Red produced promising results.

Area	**1**	**2**	**3**	**4**	**5**	**6**	**7**	**8**	**9**	**10**	**11**	**12**
GT	Bw	BW	Cvw	GWo	GWy	Gy	GOw	CWy	Wc	VWo	Vy	Vo
EST	Bw	Bw	Gbo	GOw	GO	Gbo	gowy	Gco	Wg	Vo	V	V
PSNR	27.2	25.7	32.9	32.1	31.4	30.3	32.7	40.0	41.1	43.9	31.6	33.4
ΔE_{2000}	16.7	17.5	9.9	12.2	16.7	12.9	9.4	2.6	3.8	2.1	6.3	5.4

Tab. 3. Analysis of 12 relevant areas in the case-study painting. The first two rows of the table report the ground truth and estimated labels, respectively. The highlighted columns refer to instances where the estimated labels approaches the ground truth. It is hard to correlate high values of PSNR, low values of ΔE, and accurate estimated labels.

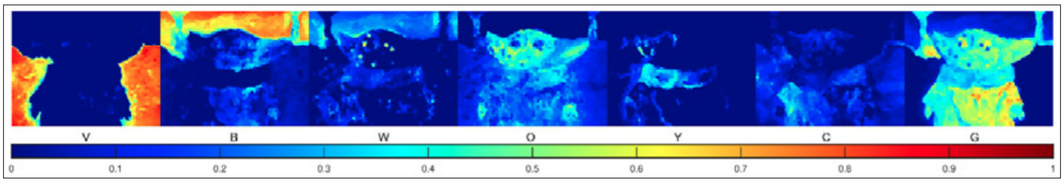

Fig. 2. Concentration maps for the case-study painting obtained inverting the purely subtractive model M2. From left to right: Vermilion, Ultramarine Blue, Kremer White, Gold Ochre DD, Naples Yellow, Novoperm Carmine Red, Viridian Green.

CONCLUSION

This research work proposed to analyze the behavior of several mixing models for pigments in an indirect fashion, by investigating their performances in a task of spectral unmixing. A set of oil painted mock-ups and a case-study painting were realized for the occasion. All the models were tried in the unmixing task of the mock-ups, and the purely subtractive model M_2 resulted the best. Such a model was later used to perform a pigment mapping task on our case-study painting, confirming its validity but also highlighting a few shortcomings in the detection of specific pigments. Our hypothesis that put in correlation a good spectral reconstruction with an accurate pigment detection was proved to stand in most of the analyzed instances, thank to the newly introduced metric *w*, which combines PSNR (spectral accuracy) and concentration error (concentration accuracy).

REFERENCES

Achanta, Radhakrishna, Appu Shaji, Kevin Smith, Aurelien Lucchi, Pascal Fua, and Sabine Süsstrunk. 2012. «SLIC superpixels compared to state-of-the-art superpixel methods.» IEEE transactions on pattern analysis and machine intelligence 34, no. 11 2274-2282.
Bioucas-Dias, José M., Antonio Plaza, Nicolas Dobigeon, Mario Parente, Qian Du, Paul Gader, and Jocelyn Chanussot. 2012. «Hyperspectral unmixing overview: Geometrical, statistical, and sparse regression-based approaches.» IEEE journal of selected topics in applied earth observations and remote sensing 5, no. 2 354-379.
Burns, Scott Allen. 2017. Subtractive Color Mixture Computation. preprint arXiv:1710.06364 , arXiv.
Deborah, Hilda, Sony George, and Jon Yngve Hardeberg. 2014. «Pigment mapping of The Scream (1893) based on hyperspectral imaging.» International Conference on image and Signal processing. Springer, Cham. pp. 247-256.
García-Bucio, María Angélica, Edgar Casanova-González, José Luis Ruvalcaba-Sil, Elsa Arroyo-Lemus, and Alejandro Mitrani-Viggiano. 2016. «Spectroscopic characterization of sixteenth century panel painting references using Raman, surface-enhanced Raman spectroscopy and helium-Raman system for in situ analysis of Ibero-American Colonial paintings.» Philosophical Transactions of the Royal Society A: Mathematical, Physical and Engineering Sciences 374, no. 2082.
George, Sony, Jon Y. Hardeberg, João Linhares, Lindsay MacDonald, Cristina Montagner, Sérgio Nascimento, Marcello Picollo, R. Pillay, T. Vitorino, and E. K. Webb. 2018. «A study of spectral imaging acquisition and processing for cultural heritage.» Digital Techniques for Documenting and Preserving Cultural Heritage pp. 141-158.
Grassi, Novella, Alessandro Migliori, PierAndrea Mandò, and Helena Calvo Del Castillo. 2005. «Differential PIXE measurements for the stratigraphic analysis of the painting Madonna dei fusi by Leonardo da Vinci.» XσRay Spectrometry: An International Journal 34, no. 4 306-309.
Grillini, Federico, Jean Baptiste Thomas, and Sony George. 2020. «Linear, Subtractive, and Logarithmic Optical Mixing Models in Oil Painting.» CVCS 2020 - Colour and Visual Computing Symposium. Gjøvik, Norway.
Jourlin, Michel, and Jean Charles Pinoli. 2001. «Logarithmic image processing: the mathematical and physical framework for the representation and processing of transmitted images.» Advances in imaging and electron physics, vol. 115 129-196.
Mantler, Michael, and Manfred Schreiner. 2000. «X-ray fluorescence spectrometry in art and archaeology.» XσRay Spectrometry: An International Journal 29, no. 1 3-17.
Naumann, Annette, Sudhakar Peddireddi, Ursula Kües, and Andrea Polle. 2007. «Fourier Transform Infrared Microscopy in Wood Analysis.» Wood production, wood technology, and biotechnological impacts 179.
Nelder, John A., and Roger Mead. 1965. «A simplex method for function minimization.» The computer journal 7, no. 4 308-313.
Pillay, Ruven, Jon Y. Hardeberg, and Sony George. 2019. «Hyperspectral imaging of art: Acquisition and calibration workflows.» Journal of the American Institute for Conservation 58, no. 1-2 3-15.
Simonot, Lionel, and Mathieu Hébert. 2014. «Between additive and subtractive color mixings: intermediate mixing models.» JOSA A 31, no. 1 58-66.
Sotiropoulou, Sophia, Zoi Eirini Papliaka, and Lisa Vaccari. 2016. «Micro FTIR imaging for the investigation of deteriorated organic binders in wall painting stratigraphies of different techniques and periods.» Microchemical Journal 124 559-567.
Strojnik, Marija, Gonzalo Paez, and Antonio Ortega. 2011. «Near IR diodes as illumination sources to remotely detect under-drawings on century-old paintings.» 22nd Congress of the International Commission for Optics: Light for the Development of the World. International Society for Optics and Photonics. vol. 8011, p. 801177.
Targowski, Piotr, and Magdalena Iwanicka. 2012. «Optical coherence tomography: its role in the non-invasive structural examination and conservation of cultural heritage objects—a review.» Applied Physics A 106, no. 2 265-277.
Yule, J. A. C., and W. J. Nielsen. 1951. «The penetration of light into paper and its effect on halftone reproduction.» Proc. TAGA, vol. 3 pp. 65-76.